

Adsorption of oxygen on clean cleaved (110) gallium-arsenide surfaces

R. Dorn, H. Lüth, and G. J. Russell*

2. Physikalisches Institut der Rheinisch Westfälischen Technischen Hochschule Aachen, Aachen, Germany

(Received 22 July 1974)

The adsorption of oxygen on clean cleaved (110) GaAs surfaces of n - and p -type material was studied by means of Auger electron spectroscopy, ellipsometry, and low-energy-electron diffraction. For both types of material a stable state of adsorption is found with an absolute coverage of approximately half a monolayer of oxygen. The sticking coefficient, which is dependent on the coverage, has different initial values S_0 for p - and n -type material (p : $S_0 \simeq 1.4 \times 10^{-6}$, n : $S_0 \simeq 3 \times 10^{-5}$). The coverage dependence of the sticking coefficient for both p - and n -type crystals is described in terms of an Elovich equation which can be derived for a thermally activated adsorption. Different bonding models for the adsorption of oxygen on the (110) surface are discussed and a qualitative interpretation of the different behavior of p - and n -type materials is given in terms of the different positions of the Fermi level at the surface.

I. INTRODUCTION

Although some of the III-V compound semiconductors have attracted considerable attention recently, little is known at present about adsorption processes on clean surfaces of these semiconductors. A study of the adsorption of oxygen on these materials is interesting for two reasons: First, oxygen is an important contaminant in technological processes; second, a lot of information is available about the oxygen adsorption on silicon surfaces,¹⁻³ and therefore a comparison of the data of these two important groups of semiconductors will be possible and should give information about some general features of oxygen adsorption on semiconducting materials.

Oxygen adsorption on GaAs has already been studied by Rosenberg *et al.*^{4,5} for vacuum-crushed samples on which, preferentially, (110) faces are exposed. These authors could distinguish between two processes: a fast chemisorption reaction and a physical reversible adsorption. The first process is also the topic of the present publication. This chemisorption process was studied volumetrically and by ellipsometry on GaP, another III-V compound, by Morgan *et al.*^{6,7} One important result of that work was the determination that the absolute saturation coverage is about 60% of an oxygen monolayer, a result which is interesting when compared with the present work on GaAs.

Oxygen adsorption on argon-bombarded and annealed polar surfaces of GaAs was studied by Arthur.⁸ Some remarkable differences between the two types of surfaces were found, and the adsorption could be shown to have a very small activation energy if it is assumed that the adsorption process is activated.

As found from previous investigations on silicon surfaces¹⁻³ the most efficient way to study adsorption processes is to combine several techniques.

Therefore in the present study Auger electron spectroscopy (AES), ellipsometry, and low-energy-electron diffraction (LEED) were used in combination. Results of electron energy-loss spectroscopy (ELS) measurements, which also contribute directly to the understanding of the present problem, have been published recently.⁹

The present measurements were performed on (110) surfaces. Clean (110) surfaces of GaAs can be prepared by cleavage in ultrahigh vacuum (UHV).

II. EXPERIMENTAL

A. Samples and UHV systems

Single crystals of n -type GaAs (Si doped with $n = 2.2 \times 10^{17} \text{ cm}^{-3}$ and $\mu = 3100 \text{ cm}^2 \text{ V}^{-1} \text{ sec}^{-1}$) and p -type GaAs (Cd doped with $p = 0.9 \times 10^{17} \text{ cm}^{-3}$ and $\mu = 210 \text{ cm}^2 \text{ V}^{-1} \text{ sec}^{-1}$) were oriented by x-ray methods and cut into a number of rectangular prisms $5 \times 5 \text{ mm}$ in cross section and 12 mm long for the AES, 8 mm long for the ellipsometric measurements. Each prism was etched in a solution of 3:1 HNO_3 :HF before being placed in an UHV-system where it was cleaved using the double-wedge technique to expose a (110) surface. Each cleavage resulted in a (110) surface of mirrorlike finish with a very low number of tear marks visible.

In the AES measurements the UHV system was a standard 360 Varian system which had a valve between ion pump and chamber as well as gas handling facilities in which spectroscopically pure oxygen and argon gases were used. The background pressure of the system was $\sim 4 \times 10^{-11} \text{ Torr}$. For the oxygen adsorption studies, the valve between pump and chamber was almost completely closed, and the exposure time was 100 sec except for exposures greater than $6 \times 10^{-1} \text{ Torr sec}$, when an oxygen pressure of $6 \times 10^{-3} \text{ Torr}$ was used. The mass spectra for the admitted oxygen gas showed that in addition to oxygen, hydrogen, argon, and

carbon monoxide (partial pressures below 1%) were also present. The oxygen pressure was read by a milli-Torr gauge placed in a bent side arm to remove any influence of the gauge. Further, the nude ionization gauge was never switched on after the crystal was cleaved.

In the ellipsometric measurements a stainless-steel chamber pumped by a turbomolecular pump (Balzer-Pfeiffer) was used. Because of the high oxygen pressures necessary for large exposures an ion pump directly attached to the chamber could not be used. Switching off and starting the ion pump would have changed the composition of the residual gas, which in this equipment consisted mainly of hydrogen. Oxygen exposure was performed as described above. Since the first detectable effects were observed at relatively high oxygen exposures a base pressure always below 10^{-9} Torr was assumed to be sufficient.

B. LEED and Auger equipment

The LEED and Auger experiments were performed using a Physical Electronics four-grid LEED system. For Auger spectroscopy the four-grid optics was used as a retarding field analyzer in conjunction with Varian Auger electronics and a phase-sensitive detector (PAR 124).

The modulation frequency was 1 kHz with a 20-V peak-to-peak modulation voltage. The lock-in preamplifier detected at 2 kHz, since the Auger spectra were recorded in the usual way as differentiated electron distributions. For the excitation a grazing-incidence electron gun was used with the crystal surface at an angle of $\sim 26^\circ$ to the primary beam direction. Auger measurements were performed with gun currents, between 50 and 200 μA , and a primary voltage of 2000 V.

C. Ellipsometry

By means of ellipsometry^{10,2} the change in the state of polarization of polarized light upon reflection at a surface is measured. Using a rotatable polarizer and a fixed quarter-wave plate, it is possible to give the incident light a state of polarization that causes the reflected light to be plane polarized. This plane of polarization can be measured by extinction using a second polarizer. In the case of extinction the settings of the two polarizers are correlated by linear equations¹⁰ to the ellipsometric angles ψ and Δ given by

$$\rho = r_p/r_s = \tan\psi e^{i\Delta},$$

where r_p and r_s are the complex reflection coefficients of the field components parallel and normal to the plane of incidence.

The ellipsometer for the present experiments consisted of a He-Ne laser (633 nm) used as a

light source, two Glan-Thomson polarizers mounted on vernier drives providing a reproducible accuracy of approximately $(10^{-2})^\circ$, a mica-plate compensator with its slow axis at 45° to the plane of incidence, and a photomultiplier as a sensitive light detector. The light was chopped at 13 Hz so that lock-in techniques could be used. The angle of incidence was fixed at 60° . Sample movement for the adjustment of the cleaved surface could be performed by means of a manipulator. A comparison of extinction settings on one surface with and without windows showed that polarization effects due to the glass windows of the UHV-chamber could be excluded. The extinction settings were found by taking the mean angle between two polarizer settings, giving equal transmitted light intensities on both sides of the minimum.

III. RESULTS

A. Auger spectroscopy

Before the adsorption study itself the clean cleaved gallium-arsenide surface was checked each time for possible contaminants. Within the sensitivity limits of AES no contamination could be detected. After each oxygen exposure, i.e., after pumping out the oxygen gas, the heights of the oxygen (509 eV), the gallium (1065 eV), and the arsenic (1223 eV) Auger peaks were recorded. For n -type material the first oxygen signals could be detected at a dosage of approximately 10^{-4} Torr sec, for p -type crystals, above 5×10^{-3} Torr sec.

During the oxygen exposure the gallium peak height changed neither for p - nor for n -type materials (Fig. 1, lower part), while the arsenic peak height for n -type crystals also remained constant.

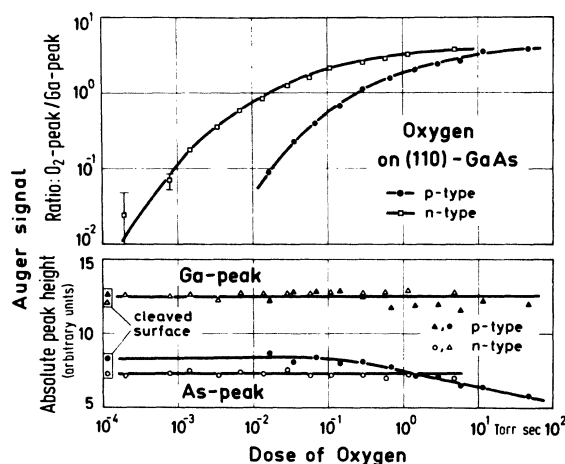


FIG. 1. Auger signal vs dose of oxygen of the adsorbed oxygen (upper part) and of the surface atoms of the underlying material (lower part).

For *p*-type surfaces, however, the arsenic peak showed a slight decrease in height for dosages higher than 10^{-1} Torr sec (Fig. 1, lower part). A different kinetics for oxygen adsorption was found for *p*- and *n*-type material: Fig. 1 (upper part) shows the ratio of the oxygen peak height divided by the constant gallium peak height to the dose of exposure. A nonlinear increase of this quantity, which is proportional to the oxygen coverage, was found and reached the same saturation value 3.8, for both *p*- and *n*-type crystal surfaces. For lower dosages the curves for *p*- and *n*-type material are displaced from each other by more than a decade, with the curve for *p*-type material being at the higher oxygen dose.

For each exposure the Auger electrons were sampled from different surface areas which had not been bombarded with electrons before exposure in order to check a possible influence of the primary beam on the adsorption process. No significant effect was found. Furthermore, exposure curves (Fig. 1, upper part) were measured with different electron-gun currents of 50, 100, and 150 μ A. The same results were obtained, i.e., the adsorption process is not affected by the primary electrons.

B. Determination of the absolute coverage

In order to measure the absolute coverage of oxygen in the saturation region of the exposure curves a comparative experiment was performed in which the adsorption of oxygen was studied simultaneously on a cleaved (111) silicon surface and a cleaved (110) gallium-arsenide surface. For the silicon surface the oxygen adsorption process is well known.^{1,2} Both surfaces were prepared in the

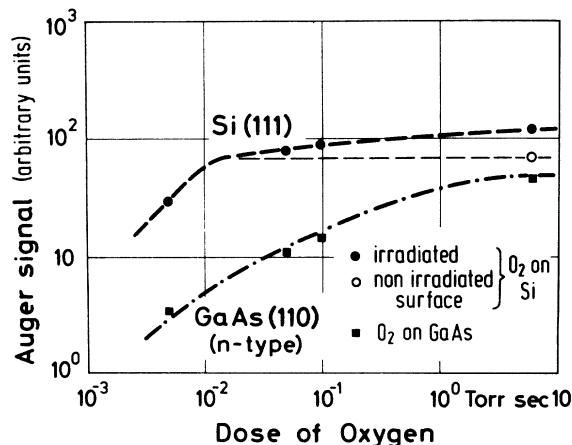


FIG. 2. Comparison of the oxygen Auger signal on a silicon (111) and a gallium-arsenide (110) surface as a function of the dose of oxygen. Both measurements were made in the same vacuum under the same conditions.

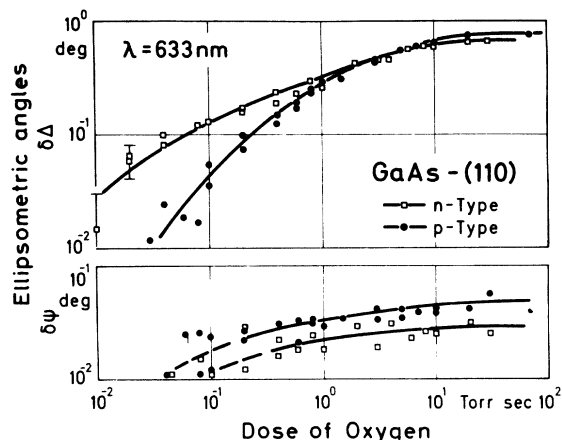


FIG. 3. Ellipsometric effect of adsorbing oxygen at a fixed wavelength of 633 nm.

same UHV. By means of a manipulator they could be brought into the primary beam at the same position and under the same angle of incidence. Figure 2 shows the absolute height of the oxygen Auger signal in arbitrary units versus exposure dose. Since measurements were performed only at a few dosages, the dotted and point-dotted lines must be taken as estimated interpolations between the data. For the silicon (111) surface the well-known second adsorption process due to electron bombardment^{1,2} can be seen; at an oxygen dose of 6 Torr sec the irradiated surface area gives a signal which is higher by a factor of 1.7 than that obtained from the nonirradiated area. This signal corresponds to a monolayer coverage, i.e., to a density of one oxygen atom per silicon surface atom.^{1,2} At the same oxygen dose the saturated-oxygen Auger signal on the gallium-arsenide surface amounts to 70% of that of the oxygen monolayer on silicon. Compared with the atom density for an oxygen monolayer on silicon this gives an absolute coverage of 5.3×10^{14} oxygen atoms per cm^2 . Related to the density of surface atoms (Ga and As) on (110) GaAs surfaces this means that the saturated adsorption phase consist of approximately 60% of a monolayer of oxygen atoms (a monolayer is two oxygen atoms for every surface molecule of GaAs).

C. Ellipsometric angles

In Fig. 3 the changes of the ellipsometric angles

$$\delta\Delta = \bar{\Delta} - \Delta \quad \text{and} \quad \delta\psi = \bar{\psi} - \psi$$

are plotted versus the dose of oxygen. $\bar{\Delta}$ and $\bar{\psi}$ are the values for the clean surfaces taken just after cleavage. Δ and ψ were determined each time after the oxygen had been pumped out of the experimental chamber. The *n*- and *p*-type samples show

a different behavior with respect to oxygen uptake both in Δ and ψ .

For the n -type crystals a nonlinear decrease of Δ is first observed at oxygen doses of approximately 1×10^{-2} Torr sec. This variation saturates at approximately 10 Torr sec. The saturation value $\delta\Delta_s$ is 0.65° . The changes of ψ could hardly be observed, because the maximal values of $\delta\psi$ were close to the limit of detection ($\sim 0.03^\circ$).

An observable decrease of Δ for the p -type crystals occurs at larger dosages (4×10^{-2} Torr sec) than for n -type material. The saturation value $\delta\Delta_s$ is 0.75° .

D. LEED observations

The clean cleaved and the oxygen-covered surfaces were also monitored by LEED after each exposure. Figure 4 shows LEED patterns of clean p - and n -type surfaces¹¹ and the same surfaces after saturation exposures with oxygen. After saturation the LEED pattern for p -type surfaces [Fig. 4(d)] did not vary markedly; only the background intensity increased, while in the case of n -type surfaces [Fig. 4(b)] the LEED pattern changed noticeably; all diffraction spots became very weak and the background intensity increased more than for p -type surfaces. Care was taken in every case that the crystal was adjusted in such a way as to avoid simulated inhomogeneous illumination of the screen.

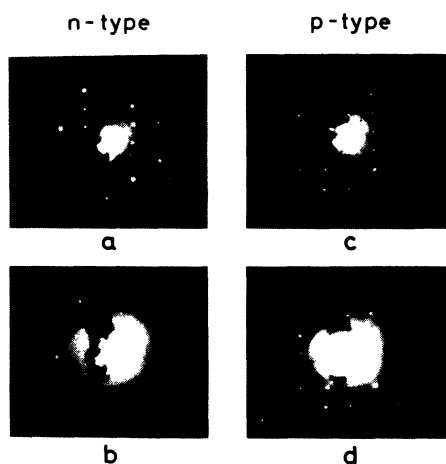


FIG. 4. LEED patterns of clean cleaved GaAs (110) surfaces, (a) and (c), and after an oxygen exposure of approximately 5 Torr sec, (b) and (d). Primary energy $E_0 = 80$ eV. The bright central spot present on each photograph is due to a misalignment of the LEED gun and optics, resulting in the gun filament being photographed. Differences between patterns (a) and (c) must be attributed to slightly different orientations of the crystals within the beam.

IV. DISCUSSION

A. Comparison of the AES and the ellipsometric results—Absolute coverage

The oxygen AES signal is directly proportional to the oxygen coverage without reference to the binding state whereas the ellipsometric changes $\delta\psi$ and $\delta\Delta$ are also influenced by the optical constants of the surface layers under consideration. Therefore a comparison of AES with ellipsometry must give some further insight into the problem.

As in previous publications^{2,12} the analysis of the ellipsometric data is performed in terms of a quasi-macroscopic-layer model, in which the surface layers are described by effective optical constants and thicknesses. The growth of an adsorbing layer then means an increase of the thickness. The anisotropy of the GaAs (110) surface is not taken into account within these model calculations. The fact that a small nonvanishing $\delta\psi$ is observed in the experiments is interpreted in a similar way to that for silicon,² as being due to a surface layer of changed optical constants n_s , κ_s (thickness d_s) present on the clean surface, which vanishes during oxygen adsorption. After saturation of $\delta\psi$ at dosages higher than 20 Torr sec the bulk optical constants of GaAs¹³ are valid up to the surface, and the surface is covered with an oxygen layer of thickness d_{O_2} . The layer present on the surface (n_s , κ_s , d_s) might be due to surface states which are compensated by the adsorbed oxygen.^{2,12}

The $\delta\Delta$ increase during adsorption depends partly on the optical constants of the growing oxygen layer and partly on those of the surface layer n_s , κ_s . The first contribution from the oxygen layer can be assumed to be linear with the oxygen coverage, whereas the second contribution might depend nonlinearly on the coverage. A nonlinear dependence of $\delta\Delta$ on the oxygen coverage is found by experiment for both n - and p -type material (Fig. 5).

If, for the adsorbed oxygen layer, a reasonable refractive index of $n_{O_2} = 1.5$ is assumed,² then, from the curves of Fig. 5 and within the framework of the present model, the refractive index n_s of the surface layer can be calculated as a function of the relative oxygen coverage Θ/Θ_s , with the thickness d_{O_2} of the adsorbed saturated oxygen layer as parameter. This is shown in Fig. 6 for d_{O_2} between 0.5 and 6 Å. The quantity n_s decreases monotonically with coverage or exhibits a maximum, depending on the thickness of the oxygen layer. Since only a monotonic decrease of n_s with increasing oxygen coverage is reasonable, the effective thickness of the oxygen layer after saturation should not exceed 1 Å. A monolayer of oxygen is expected to have a thickness of about 2 Å (correspondent to a bonding length of about 1.6 Å). The absolute coverage therefore is estimated to be

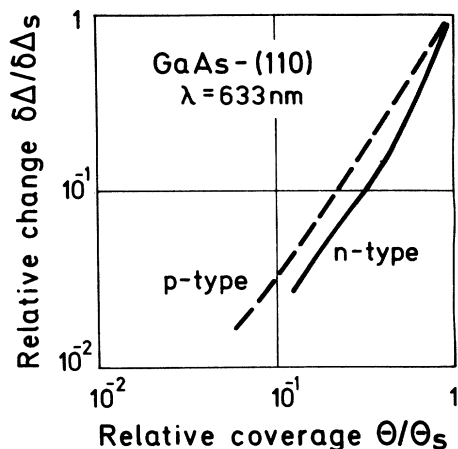


FIG. 5. Dependence of the relative change of the ellipsometric angle $\delta\Delta$ on the relative oxygen coverage. Θ_s refers to the saturation coverage of approximately 60% of a monolayer.

nearly half a monolayer in good agreement with the experimental result (Sec. III B).

The theoretical analysis of the ellipsometric data, therefore, is consistent with the experimental determination of the absolute oxygen coverage within the first saturated state of adsorption. Neither from this theoretical analysis nor from the experimental determination (Sec. III B) it is possible to decide if the absolute coverage is exactly half a monolayer or if the experimental value of 60% of a monolayer is exact. A margin of error of approximately $\pm 10\%$ must be taken into account. Since the analysis is based on a continuum model, no conclusions can be drawn from ellipsometry concerning the atomic structure of the adsorbate.

B. Discussion of the sticking coefficient

Besides the absolute coverage, the other important parameter for the description of the adsorption kinetics is the sticking coefficient S defined by

$$\frac{d\Theta}{dt} = S(\Theta) \frac{\nu p}{N_0} \quad (1)$$

Θ is the fractional coverage related to a monolayer of oxygen; i. e., $\Theta_s = 0.6$ (corresponding to 5.3×10^{14} atoms/cm²) gives the fractional coverage after saturation of the first adsorption process under consideration. For the calculation of N_0 , the number of surface sites for a molecule, an absolute saturation coverage of $\Theta_s = 0.6$ (Sec. III B) is assumed; i. e., $N_0 = 2.65 \times 10^{14}$ molecules/cm², p is the pressure, and $\nu = 3.48 \times 10^{20}$ (molecules/cm² Torr sec) is the number of molecules that strike unit area of the surface per unit time and unit pressure at 300 °K. By differentiation of the AES coverage versus oxygen dose curves (Fig. 1), the

sticking coefficient $S(\Theta)$ as a function of coverage is derived (Fig. 7). The sticking coefficients for zero coverage approach the values $S_0^{(n)} = 3 \times 10^{-5}$ and $S_0^{(p)} = 1.4 \times 10^{-6}$, which can better be seen from a double logarithmic plot. For both n - and p -type materials the sticking coefficient exhibits a nearly exponential coverage dependence over a large range of Θ . The curves can be fitted to a type of Elovich equation¹⁴ (Fig. 7)

$$S = S_0 \frac{Z(1 - \Theta/\Theta_s)^2}{Z - \Theta/\Theta_s} e^{-(E_0 + \beta\Theta/\Theta_s)/kT}, \quad (2)$$

with

$$\beta = 7.7 \times 10^{-2} \text{ eV and } Z = 4$$

This mathematical description implies the assumption of an activated adsorption process in which the activation energy depends linearly on the coverage. This is reasonable if every adsorbing molecule gives rise to a further increase of the potential barrier E_0 present on the surface. The function

$$f(\Theta) = Z(1 - \Theta/\Theta_s)^2 / (Z - \Theta/\Theta_s) \quad (3)$$

describes the probability that a gas molecule collides with a vacant site to be adsorbed. The special form (3) is valid for an immobile adsorption layer.¹⁴ The exact shape of $f(\Theta)$ does not have much influence on the fit. With small changes in β other types of $f(\Theta)$ functions can also be chosen e. g., for mobile layers. Also Z , the number of

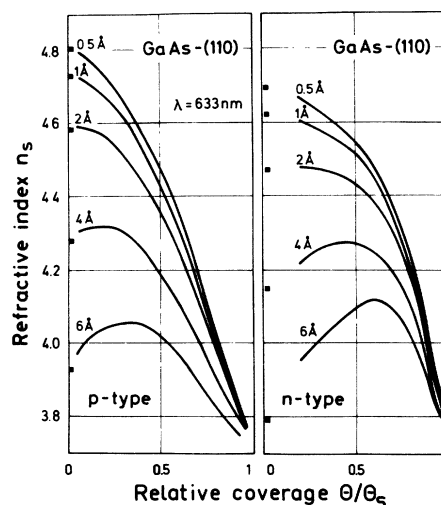


FIG. 6. Refractive index n_s of a surface layer present on the clean surface with changed optical constants as a function of the relative oxygen coverage. The thickness of the adsorbed oxygen layer after saturation is given as a parameter (in Å). The curves are obtained from a model calculation in order to describe the ellipsometric results.

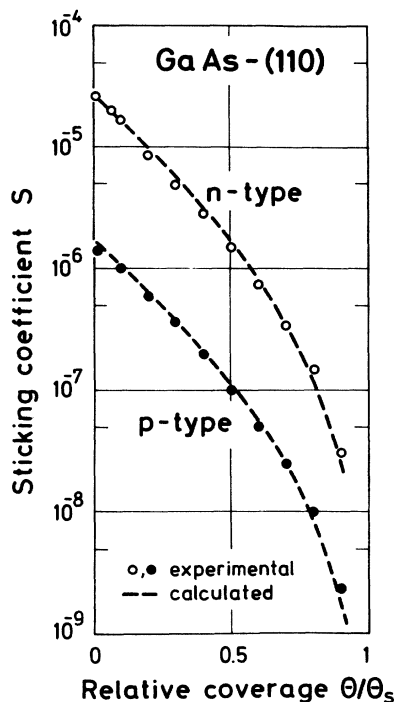


FIG. 7. Sticking coefficient S as a function of the relative oxygen coverage. $\Theta/\Theta_s = 1$ refers to saturation at approximately 60% of a monolayer. The calculated curves are obtained from a fit of an Elovich equation to the experimental results.

neighbors surrounding a site ($Z = 4$ in the present fit), can be changed to some extent without any important effect. Therefore $f(\Theta)$ does not give much insight into the adsorption problem.

The accommodation coefficient σ is dependent on the ratio of the partition functions for the adsorbed and for the free-gas molecule.¹⁴ Its value depends on the degrees of freedom of the adsorbed atoms or molecules. The interpretation of the adsorption in terms of an activated process is also suggested by a comparison with the measurements by Rosenberg *et al.*⁵ on crushed samples at 78 °K. They find a fast reaction (chemisorption) comparable with the present one which stops at higher dosages than found in our experiments. For an activated adsorption this is expected owing to the lower temperature used. Also a saturation coverage of about half a monolayer is found by these authors. A quantitative comparison of the results of Rosenberg *et al.* with the present ones in order to determine the constant part E_0 of the activation energy was not possible owing to uncertainties concerning the sticking coefficients and the type of material used by these authors. Therefore only the product $\sigma e^{-E_0/kT}$ can be obtained from the present experiments and it is found to be 3×10^{-5} for n -type and

1.4×10^{-6} for p -type material. At present it is not possible to decide if the different absolute values of the sticking coefficient for p - and n -type materials must be explained by different activation energies $E_0^{(n)}$, $E_0^{(p)}$, and/or different values $\sigma^{(n)}$, $\sigma^{(p)}$. A rough estimation for an upper limit for the constant term E_0 of the activation energy is possible since, for oxygen, calculated values of σ are known¹⁴: For mobile adsorption complexes, $\sigma^{(n)}$ and $\sigma^{(p)}$ must be about 1 (with no loss of rotation, 300 °K) or about 0.1 (with loss of one rotation, 300 °K). For immobile complexes, $\sigma^{(n)}$ and $\sigma^{(p)}$ must have values between 10^{-4} and 3×10^{-2} .¹⁴

With the assumption that the differences between p - and n -type materials must be attributed to different terms $E_0^{(n)}$, $E_0^{(p)}$, the following estimations are valid:

$$\left. \begin{array}{l} 0.2 < E_0^{(n)} < 0.26 \text{ eV} \\ 0.28 < E_0^{(p)} < 0.33 \text{ eV} \end{array} \right\} \text{mobile complexes,}$$

$$\left. \begin{array}{l} 0.03 < E_0^{(n)} < 0.07 \text{ eV} \\ 0.11 < E_0^{(p)} < 0.25 \text{ eV} \end{array} \right\} \text{immobile complexes.}$$

The upper limit therefore is $E_0 \leq 0.33$ eV. No comparable results are known to the authors at present. Only from the work of Arthur⁸ on polar surfaces can an estimated upper limit of the activation energy be given: $E_0 < 8$ kcal/mole; i. e., $E_0 < 0.3$ eV, in agreement with the estimation for (110) surfaces of the present work.

C. Bonding models

The different initial sticking coefficients for n - and p -type crystals should be correlated to the different positions of the Fermi level at the surface, about 0.6 eV for n -type and about 0.08 eV for p -type material, respectively, above the valence-band edge.¹⁵ But photoemission work performed by Gregory *et al.*¹⁶ does not show any occupied surface states within the lower half of the forbidden band gap, which could explain the difference in sticking coefficients. A possible explanation is that on n -type crystals surface states in the upper-half of the forbidden band gap, as suggested by Gregory *et al.*¹⁶ are filled to a small extent with electrons which can induce a chemical bond to the oxygen at dosages lower than those where the main adsorption process due to the completely occupied deep-lying surface levels (within the valence-band energy range¹⁶) starts. On p -type material these surface states within the upper-half of the forbidden bands are completely empty and cannot form these additional oxygen bonds. Since for both n - and p -type materials the same saturation coverage of about half a monolayer is reached, the limiting factor for the adsorption process must be determined by the geometry of the chemical bond be-

tween oxygen and surface atoms (Fig. 8).

Several models for the adsorption of oxygen on clean (110) GaAs surfaces are discussed in the literature. From the analysis of electron-paramagnetic-resonance measurements Miller and Hane-man¹⁷ are led to the assumption that oxygen is adsorbed at liquid N₂ temperatures as O₂⁻ molecules which are bonded only to the Ga-atom (Fig. 8). This model does not explain the present room-temperature results, for saturation coverage would be reached with one monolayer of oxygen atoms (per surface atom) unless the Fermi-level position is the determining factor for the saturation. But in that case the experimental result that the saturation coverages of about half a monolayer on *p*- and *n*-type surfaces are equal cannot be understood.

Rosenberg *et al.*⁵ who have studied oxygen adsorption on vacuum-crushed powders of GaAs, have discussed two bonding models which are consistent with a half-monolayer coverage:

(i) an H₂O-like bond of one oxygen atom with two next-neighbor surface atoms of different kinds,

(ii) a peroxide bridge configuration in which an O₂ molecule is bonded with two next-neighbor surface atoms of the same kind. Both configurations might be possible as far as bonding angles and bonding lengths are concerned, but in case (ii) the surfaces mesh (Fig. 8) is expected to be changed. This is not observed in the experiments, the LEED patterns after oxygen adsorption [Figs. 4(b) and 4(d)] do not show any superstructure.

A recent approach to the problem which is based on theoretical calculations of surface states on the

clean (110) GaAs surface and on photoemission data on the clean and oxygen-covered surfaces has been given by Gregory *et al.*¹⁶ On the clean surface two types of surface states are assumed: one filled band formed by As orbitals (two excess electrons per As surface atom) within the energy range of the valence band and another nearly empty band formed by Ga orbitals which lies in the upper-half of the forbidden band gap and which is responsible for the pinning of the Fermi level on *n*-type material. The chemical bond to the adsorbed oxygen is performed by the filled As levels. The authors therefore are led to the assumption that an adsorbed oxygen atom is bonded preferentially to the As surface atoms (half a monolayer), while leaving the empty Ga levels largely unaffected. At least for *p*-type material this model is in agreement with the results of the present work as far as LEED observation and total coverage are concerned. The assumption of a preferential oxygen bond to the As surface atoms is also supported by recent investigations of the oxygen adsorption on the polar (111) GaAs surfaces. Ranke and Jacobi¹⁸ find an initial sticking coefficient of about 10⁻³ for oxygen on the (111) As face and of about 10⁻⁴, respectively, for the (111) Ga face.

For *n*-type surfaces recent observation of an additional characteristic oxygen electronic transition in electron-energy-loss measurements⁹ (not present on *p*-type material) and the LEED studies of the present work suggest the existence of an additional type of oxygen bonding on *n*-type surfaces compared to *p*-type material. This could be due to a small contribution of electrons within the nearly empty Ga levels forming an additional bond of the type Ga-O-As, which is irregularly spread over the surface. This would decrease the degree of order within the adsorbed species, as is observed in the LEED patterns [Fig. 4(b)]. Furthermore, if the small decrease in the As Auger peak height for high oxygen dosages observed on *p*-type surfaces (Fig. 1) is attributed to a penetration effect, it seems reasonable that on *n*-type material this decrease starts at higher dosages, as indicated in Fig. 1, because As surface atoms are shielded to a lesser extent if a Ga-O-As type of bonding is also formed.

From the present results the two possibilities cannot be distinguished between: irregularly spread domains of Ga-O-As bonds or an amorphous Ga-O-As layer in which Ga and As are no longer a part of the GaAs (110) lattice. Also an additional mobile adsorption phase of oxygen on *n*-type material might be taken into account.

V. CONCLUSION

At the present state of knowledge an unequivocal bonding model for oxygen on clean (110) gallium-

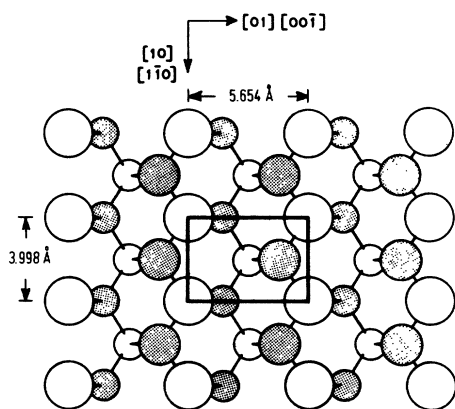


FIG. 8. Schematic drawing of the GaAs structure as viewed along the (110) direction. Shaded circles: atoms of one kind, say Ga atoms; unshaded circles: those of the other kind, say As atoms. The relative sizes of the two types of circles are an indication of depth into the crystal, the small circles being situated in deeper layers. The (1×1) unit mesh is marked within the uppermost lattice plane.

arsenide surfaces cannot be presented, but the surface state model of Gregory *et al.*¹⁶ allows an understanding of the experimental facts presented in this work. Further experimental data are needed; in particular, information concerning the vibration states of the adsorbed oxygen would be useful, as would be further experiments to prove the surface-state model suggested by Gregory *et al.*¹⁶

ACKNOWLEDGMENTS

The authors wish to thank Professor G. Heiland for helpful discussions and critical reading of the manuscript. Also discussions with Professor W. E. Spicer are gratefully acknowledged. The work was financially supported by the Deutsche Forschungsgemeinschaft in the SFB 56, Aachen. The numerical calculations were performed at the Rechenzentrum of the RWTH Aachen.

*Present address: School of Physics, The University of New South Wales, Sydney, 2033, N.S.W., Australia.

¹H. Ibach, K. Horn, R. Dorn, and H. Lüth, *Surf. Sci.* **38**, 433 (1973).

²R. Dorn, H. Lüth, and H. Ibach, *Surf. Sci.* **42**, 583 (1974).

³H. Ibach and J. E. Rowe, *Phys. Rev. B* (to be published).

⁴A. J. Rosenberg, *J. Phys. Chem. Solids* **14**, 175 (1960).

⁵A. J. Rosenberg, J. N. Butler, and A. A. Meena, *Surf. Sci.* **5**, 1 (1966).

⁶W. J. M. Van Velzen, and A. E. Morgan, *Surf. Sci.* **39**, 255 (1973).

⁷A. E. Morgan and W. J. M. Van Velzen, *Surf. Sci.* **40**, 360 (1973).

⁸J. R. Arthur, *J. Appl. Phys.* **38**, 4023 (1967).

⁹H. Lüth and G. J. Russell, *Surf. Sci.* (to be published).

¹⁰F. L. McCrackin, E. Passaglia, R. R. Stromberg,

and H. L. Steinberg, *J. Res. Natl. Bur. Stand. A* **67**, 363 (1963).

¹¹A. U. MacRae and G. W. Gobeli, *J. Appl. Phys.* **35**, 1629 (1964).

¹²F. Meyer, E. E. de Kluizenaar, and G. A. Bootsma, *Surf. Sci.* **27**, 88 (1971).

¹³H. R. Philipp and H. Ehrenreich, *Phys. Rev.* **129**, 1550 (1963).

¹⁴D. O. Hayward and B. M. W. Trapnell, *Chemisorption*, 2nd ed. (Butterworths, London, 1964), pp. 67–107.

¹⁵J. H. Dinan, L. K. Galbraith, and T. E. Fischer, *Surf. Sci.* **26**, 587 (1971).

¹⁶P. E. Gregory, W. E. Spicer, S. Ciraci, and W. A. Harrison (unpublished).

¹⁷D. J. Miller and D. Haneman, *Phys. Rev. B* **3**, 2918 (1971).

¹⁸W. Ranke and K. Jacobi, *Surf. Sci.* (to be published).

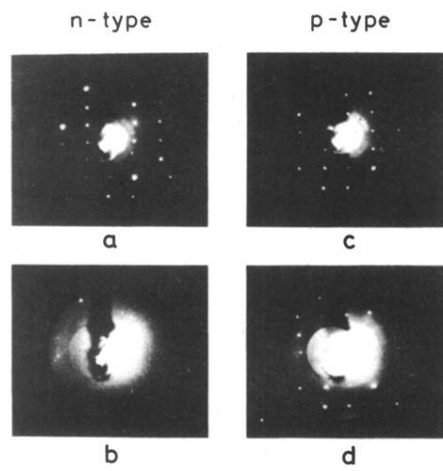


FIG. 4. LEED patterns of clean cleaved GaAs (110) surfaces, (a) and (c), and after an oxygen exposure of approximately 5 Torr sec, (b) and (d). Primary energy $E_0 = 80$ eV. The bright central spot present on each photograph is due to a misalignment of the LEED gun and optics, resulting in the gun filament being photographed. Differences between patterns (a) and (c) must be attributed to slightly different orientations of the crystals within the beam.

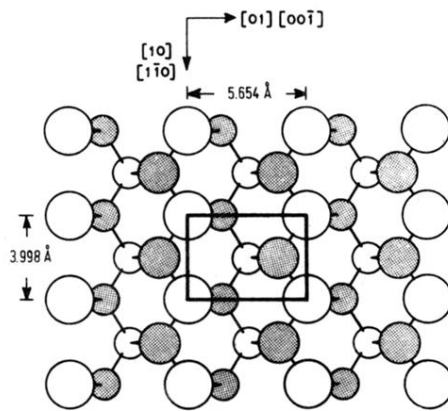


FIG. 8. Schematic drawing of the GaAs structure as viewed along the (110) direction. Shaded circles: atoms of one kind, say Ga atoms; unshaded circles: those of the other kind, say As atoms. The relative sizes of the two types of circles are an indication of depth into the crystal, the small circles being situated in deeper layers. The (1×1) unit mesh is marked within the uppermost lattice plane.